

Zinc and graphene oxide composites as new protective coatings for oil and gas pipes

M. Sajid Ali Asghar¹⁾ (ORCID ID: 0000-0002-4551-1299), Muhammad Amir^{2), *} (0000-0001-5513-053X), Umer Hussain¹⁾ (0009-0004-8293-492X), Mohammed M. Sabri³⁾ (0000-0001-9375-7202)

DOI: <https://doi.org/10.14314/polimery.2023.7.3>

Abstract: A method was developed to obtain a durable coating consisting of zinc and graphene oxide (Zn-GO) in order to reduce the mechanical wear and tear rate of oil and gas pipelines made of steel. Graphene oxide was obtained from graphite by wet chemical oxidation (unmodified and modified Hummers' method) using potassium permanganate and sulfuric acid. The process was carried out at various temperatures. The steel was covered with an ultrathin layer of Zn-GO using the electrophoretic deposition method. The GO particle size (< 90 nm) was confirmed by XRD and laser analysis. For GO particles obtained by the modified Hummers' method, a significant correlation was observed in the scratch ($R^2 = 0.87$) and the Vickers microhardness tests ($R^2 = 0.93$), which indicates a lower wear rate of Zn-GO-coated steel.

Keywords: corrosion resistance, graphene oxide, Hummers' method, nanocomposites, electrophoretic deposition.

Kompozyty cynku i tlenku grafenu jako nowe powłoki ochronne rur do przesyłu ropy i gazu

Streszczenie: Opracowano metodę otrzymywania trwałej powłoki składającej się z cynku i tlenku grafenu (Zn-GO) w celu zmniejszenia zużycia mechanicznego rurociągów naftowo-gazowych wykonanych ze stali. Tlenek grafenu pozyskano z grafitu metodą mokrego utleniania chemicznego (niezmodyfikowana i zmodyfikowana metoda Hummersa) z użyciem nadmanganianu potasu i kwasu siarkowego. Proces prowadzono w różnej temperaturze. Stal powlekaną ultra cienką warstwą Zn-GO techniką osadzania elektroforetycznego. Metodą XRD i analizą laserową potwierdzono wielkość cząstek GO (≤ 90 nm). Dla cząstek GO otrzymanych zmodyfikowaną metodą Hummersa zaobserwowano znaczącą korelację w teście zarysowania ($R^2 = 0.87$) i mikrotwardości Vickersa ($R^2 = 0.93$), co świadczy o mniejszym stopniu zużycia stali pokrytej powłoką Zn-GO.

Słowa kluczowe: odporność na korozję, tlenek grafenu, metoda Hummersa, nanokompozyty, osadzanie elektroforetyczne.

Pakistan is rich in natural resources and its economy is growing at an annual rate of 2.7 percent [1]. An increase in energy demand making the oil and gas industry which are world most influential industries. Recognizing the centrality of oil and gas pipelines in nowadays energy distribution system, ensuring that they continue to function safely is a top priority for the gas and oil industries and their supply chains [1]. Metallic oil and gas pipelines assemblies have been damaged by mechanical wear and

tear and corrosion related failures. In oil and gas industry, 25% of all failure is due to corrosion, with pipeline corrosion accounting for more than 50% of all failures [2]. Failure depends on the operational environment and installation site, as well as age. Oil and gas pipelines are susceptible to a variety of degradation processes due to mechanical wear and tear, corrosive wear, cracks, leaks and pipeline wall thinning [3].

The increase in demand for energy makes the oil and gas industry the most influential industry in the world [1]. In the oil and gas industry, 25% of all failures are due to corrosion, with pipeline corrosion accounting for more than 50% of all failures [1, 2]. Failure depends on the operating environment and installation location, as well as its lifetime. Oil and gas pipelines are susceptible to various degradation processes due to mechanical wear, corrosive wear, cracks, leaks, and wall thinning of pipelines [3].

¹⁾ Materials Engineering Department, NED University of Engineering and Technology, Karachi, Pakistan.

²⁾ Textile Engineering Department, NED University of Engineering and Technology, Karachi, Pakistan.

³⁾ Department of Physics, Faculty of Science and Health, Koya University, Koya KOY45, Kurdistan Region - F.R., Iraq.

* Author for correspondence: qureshi@neduet.edu.pk

Mechanical wear is responsible for quarter of all failures, while half of all failure is due to sweet and/or sour corrosion in pipelines [4, 5]. This mechanical wear and tear lead to fatal catastrophes, resulting in loss of lives in the worst cases. Pipeline failure is due to material erosion, corrosive wear, wear and tear and an equipment failure, while causes of oil and gas pipeline failure are archaeological damage and corrosion [3, 6]. This substantial threat in oil and gas products demands comprehensive knowledge of the mechanism of failures as well as evaluation and management measures [7].

To address the discussed failures, established knowledge provides the remedial action with certain limitation. Graphene has water repellent properties and possesses remarkable chemical inertness [8]. A graphene coating, whether it is a single layer or multiple layers on metal, can significantly improve mechanical strength and corrosion resistance which can be estimated by up to 1.5 orders of magnitude [9]. It was established, that graphene has provided extremely viable solution for corrosion resistance [10]. The basic requirements for an ideal surface barrier against corrosion are: providing immunity to materials from degradation in chemically aggressive environments, to resist permeation of corrosive fluid and mechanical integrity over the anticipated life of treated parts [10, 11].

The graphite consists of flat hexagonal rings owing to its planar and layered structure. In every single layer, carbon atoms are orchestrated in a honeycomb matrix structure having interatomic separation and inter-plane separation of 0.142 nm and 0.335 nm, respectively [12]. However, graphene is a crystalline polymorph of carbon with 2D properties. In this structure carbon atoms are tightly packed with each carbon atom producing four bonds. Among four bonds, one bond is with each of its three neighboring atoms, while the fourth bond is located vertically to the lattice plane [13]. It is worth mentioning that graphene has a good tensile strength because of their covalent bonding with the bond length of 1.42 Å [12, 14]. High tensile strength and surface to volume ratio of graphene has good impact in fabricating nanocomposites [14].

The development of graphene nanocomposites is a cycle of creating or separating graphene of the desired size, shape, and purity of the explicit product [5]. There are two methodologies to produce graphene nanoparticles. Firstly, top-down methodology which includes micromechanical exfoliation [15] (Scotch Tape), chemical exfoliation and chemical synthesis. The latter also includes (i) Hummers' and Offeman and (ii) modified Hummers' method. Secondly, bottom-up methodology which includes epitaxial growth, pyrolysis and chemical vapor deposition (CVD) [16].

The present research is focused on controlling oil and gas pipeline mechanical wear and tear and corrosion by using sustainable zinc-graphene oxide composite coating. Coating has beneficial properties, including the capability of suppressing corrosion, change conductiv-

ity, improve wear, increase bonding strength, prevent chafing, increase high thermal stability, and increase the hardness of the material [17]. Coating techniques directly alter the characteristics and functions of a material and enhance the life of coated material [18]. Oil and gas pipelines are subjected to harsh environments where they undergo corrosion at a very rapid rate. The corrosion of pipelines results in the loss of material as well as affecting the purity level of the fuel [19]. Coating technique is one of the finest techniques used to prevent mechanical wear and tear and corrosion of the gas and oil pipelines [18–20]. Appropriate coating technique will protect pipelines from getting a mechanical wear and tear and corrosion. In general, several types of coating; electrophoretic deposition, chemical vapor deposition, solution dip coating of polymers and electrophoretic deposition are reported [16, 21, 22]. Electrophoretic deposition coating provides an improved material's surface properties and developed new material surface for further advanced applications [15, 23, 24, 29]. It has been reported that Zn has long been used as a coating material in corrosive environments for metal preservation. The anti-corrosion properties of zinc result from its anodic tendency to sacrifice when it interacts with iron [19]. Due to the fact that the potential of zinc is more negative (1050 mV/SCE) [30] than that of steel (650 mV/SCE) [31] under the same conditions (3.5 wt. % NaCl solution), zinc deposits function as sacrificial anodes and provide cathodic protection for A-36 class steel.

The aim of this work was to develop a durable composite coating of zinc and graphene oxide (Zn-GO) that would reduce the mechanical wear of oil and gas pipeline materials (A-36 grade steel). GO was obtained from graphite by wet chemical oxidation (Hummers', and modified Hummers' methods). Steel type A-36 was coated with an ultra-thin layer of Zn-GO by electrophoretic deposition technique. This technique uses an electric current to reduce the number of cations (zinc) of a selected material (GO nanoparticles) from an electrolyte solution (zinc sulfate) and apply a nanocomposite coating in a thin layer to the conductive surface of A-36 mild steel, which significantly improves the morphology of the coating [19, 20, 25]. XRD and laser analyses were used to determine the size of GO nanoparticles. The durability of the Zn-GO coating was determined using the scratch coefficient and Vickers hardness.

EXPERIMENTAL PART

Material

A cracked electrode from an electric arc furnace was used as a source of 99% pure graphite. Sodium nitrate (NaNO_3 , 99%), sulfuric acid (H_2SO_4 , 99%), potassium permanganate (KMnO_4 , 99%), hydrogen peroxide (H_2O_2 , 50%) were purchased from Sigma Aldrich. Hydrochloric acid (HCl , 99%), zinc sulfate ($\text{ZnSO}_4 \cdot 7\text{H}_2\text{O}$, 99%), sodium

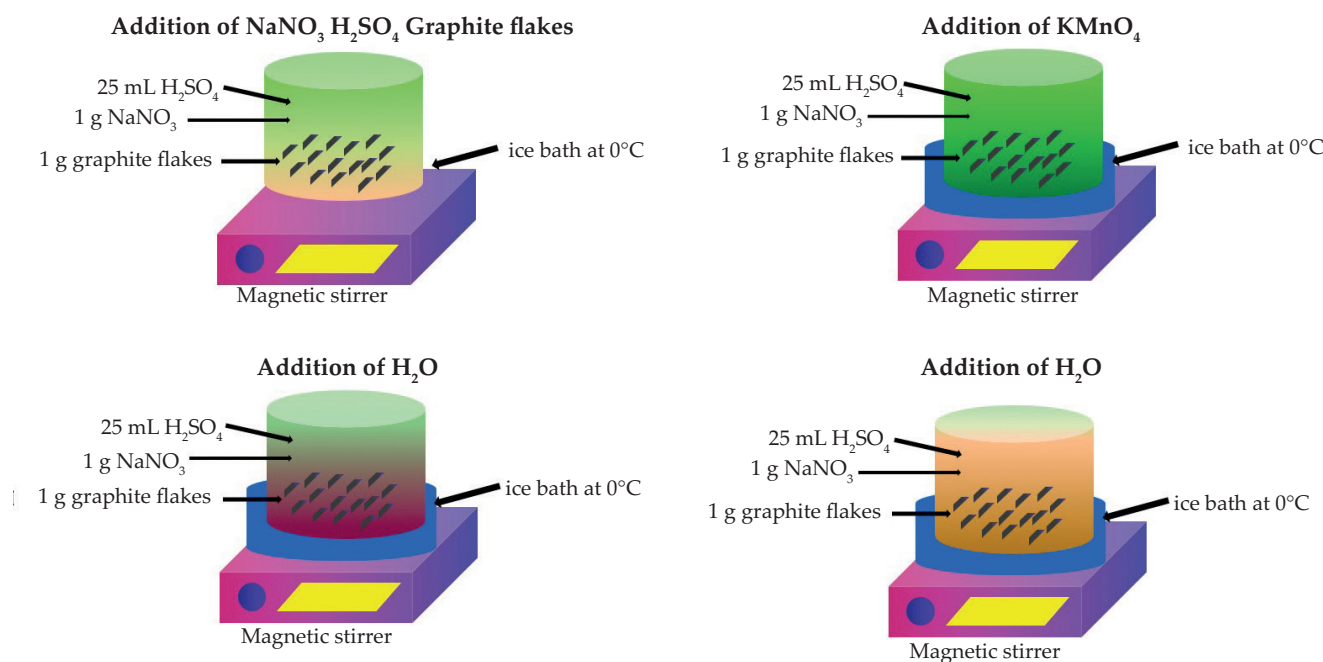


Fig. 1. Synthesis steps of GO using Hummers' methods [15]

Table 1. Chemical composition of A-36 steel

Chemical	S	Mn	C	Si	Cu	Fe
wt%	0.05	1.03	0.27	0.28	0.20	98.0

sulfate (Na_2SO_4 , 99%), and sodium chloride (NaCl , 99.99%) were supplied by Merck. Grade A-36 mild steel, which is used for oil and gas pipelines, was selected and its chemical composition was investigated by OES spark spectroscopy technique (SpectroMAXx, Germany) as shown in Table 1.

GO synthesis by Hummers' method

Nano sized graphene oxide particles were prepared *via* Hummer's and modified Hummers' method (Fig. 1).

In this research, Hummers' method was opted for the synthesis of nano sized graphite oxide (Fig. 2). Graphite powder was obtained by drilling through the graphite electrode. The obtained amount of powder was then measured using an electronic precision scale. To the beaker were added 1 g of graphite powder, 1 g of NaNO_3 and 25 mL of 99% H_2SO_4 and was stirred in ice bath at 0°C for two hours. Then, 3 g of KMnO_4 was added slowly, followed by one hour stirring in ice bath at a temperature below 20°C . After one hour, the beaker was removed from ice bath and warmed up until mixture reached room temperature. In the next step, 100 mL of distilled water was added to the beaker, followed by stirring for two days at 35°C . After that time, 200 mL of distilled water and 10 mL of H_2O_2 was added to finish the reaction, as was evident by the change in color of the precipitate from brown to yellow [8].

For GO synthesis magnetic stirrer, centrifuge machine (TG-16, China) and sonication (FSF-010S, Faithful, China) equipment were used.

GO synthesis by modified Hummers' method

5 g of NaNO_3 and 115 mL of H_2SO_4 was added into a beaker, then mixed for 10 min by magnetic stirrer at 0°C . After 10 min, 15 g of KMnO_4 was gradually added, then stirred for 20 min at 10°C . In the next step, mixture was heated up to 35°C and stirred for 30 min. To terminate the reaction and remove the excess of KMnO_4 , 10 mL of H_2O_2 was added. The exothermic reaction occurs and to lower the temperature 230 g of ice was added to the mixture and stirred for 15 min [26].

Post processes of developed GO nanoparticles

Centrifuge and purification

The centrifugation process of the obtained samples was the same regardless of the method used. The mixtures were washed by adding 10 mL of 35% HCl solution and centrifuged in a laboratory centrifuge (TG 16, China) at a speed of 500–1000 rpm for 30 min. Then 100 mL of distilled water were added and centrifuged again. The purification process was continued until the pH of the



Fig. 2. GO synthesis: a) obtaining graphite flakes, b) weighing, c) before reaction, d) centrifuge, e) after centrifugation, f) dryer, g) vacuum filtration, and h) ultrasonic exfoliation

solution was neutral. Table 2 summarizes the pH data for samples prepared using the Hummer' method and the modified Hummer' method, respectively.

Drying and vacuum filtration

After purification, the obtained purified and rinsed GO was oven dried at 100°C for 3 h. After drying, vacuum filtration method was used for separating GO and other residue or solid from a remaining liquid, as shown in Figure 2g.

Sonication

Finally, cost-effective graphite exfoliation method was exercised for generating of high-quality graphene sheets

on a large scale by sound waves at 50 Hz using ultrasonic bath (FSF-010S, Faithful, China). This technique allows you to easily obtain large amounts of pure graphene. To prevent sample heating up during and after the sonication process, ice cubes was utilized [26, 27].

Electrophoretic deposition

The Zn-GO composite was deposited on a sample of A-36 steel by electrophoretic deposition. In the electrophoretic method, galvanization was performed using electric current in an electrolyte solution (Table 4). Figure 3 shows the electrodeposition setup. When current flows through the system, metal ions from the electrolyte are reduced and deposited as a thin layer on top of one of the electrodes, causing it to be electroplated. An appropri-

Table 2. The pH data of Hummers' and modified Hummers' methods

Washing cycle	Speed, rpm	Time, min	pH value	
			Hummers' method	Modified Hummers' method
1 st	500	30	1.25	1.10
2 nd	800	30	2.25	2.20
3 rd	800	30	3.10	3.00
4 th	800	30	3.75	3.90
5 th	1000	30	3.92	4.50
6 th	1000	30	4.70	4.90
7 th	1000	30	5.90	5.00
8 th	1000	30	6.42	5.98
9 th	1000	30	6.99	7.00

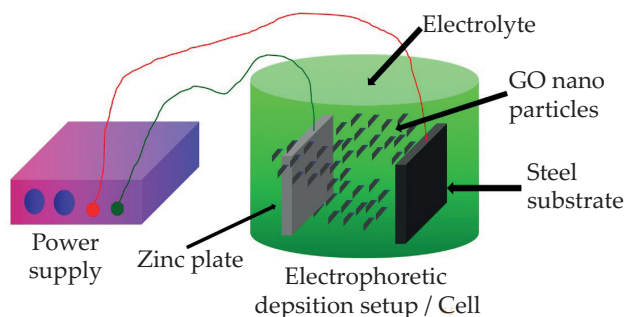


Fig. 3. Electrodeposition setup

ate sample preparation method was used before coating. In the first stage, the steel sample was rinsed with distilled water and polished with 180-mesh sandpaper. In the second stage, the sample was immersed in concentrated 12 M hydrochloric acid for 30 seconds. After rinsing the sample with distilled water, 1M sodium hydroxide solution was used to neutralize the remaining acid.

Methods

X-ray diffraction (Xpert PRO, Panalytical Company, Netherlands) was used to evaluate the average number of graphene oxide layers and crystal size, with a 2θ angle, varying between $10\text{--}80^\circ$ and a wavelength of 1.54 \AA at a voltage and a current of 40 kV and 30 mA, respectively. Laser particle analyzer (Mastersizer3000, Malvern, UK) was used to determine the distribution of GO nanoparticles as a function of bulk density. Scratch test (ST30, Teer, UK) and Vickers microhardness (402MVD, Wolpert,

Germany) were used to observe the effectiveness of developed Zn-GO nanocomposite coating on steel. The electrophoretic deposition was conducted at room temperature for 30 minutes. Using a dilute H_2SO_4 solution, the pH of the solution was kept at 5 pH. The plating bath was mechanically agitated for 2 hours and ultrasonically for 1 hour before electrophoretic to achieve homogeneous dispersion of GO in the plating bath solution. The electrolyte bath composition and the electrophoretic coating operation parameters are presented in Table 3.

RESULTS AND DISCUSSION

X-ray diffraction analysis

According to [29], XRD analysis shows that GO is formed at $2\theta = 12^\circ$. Reduced graphene oxide is formed during the oxidation of graphite into graphite oxide at $2\theta = 12^\circ$ and the peak between $2\theta = 18^\circ$ and $2\theta = 20^\circ$ is associated with KMnO_4 and the peak $2\theta = 26.7^\circ$ is related to unreduced graphite. X-ray diffraction pattern (Fig. 4), graphite reflects characteristic peak at $2\theta = 26.7^\circ$. After the introduction of oxygen functionalities, the graphitic peak shifts to $2\theta = 11.55^\circ$, which was a typical XRD of graphite that exhibits a sharp diffraction peak at $2\theta = 26^\circ\text{C}$, which was mainly due to the presence of a huge amount of carbon with oxygen, thus showing the presence of graphite oxide being expressed by the height of the peak.

Graphite shows a fundamental diffraction peak at $2\theta = 11.56^\circ$ (d spacing = 7.66 \AA), which was caused by the oxidation of graphite and indicates that the graph-

Table 3. Process parameters of electrolyte set up

Electrolyte		Electroplating	
Bath composition	Concentration, g/L	Parameter	Value
$\text{ZnSO}_4 \cdot 7\text{H}_2\text{O}$	180	Current density	10 mA/cm^2
Na_2SO_4	30	Deposition time	0.5, 1, 2, 2.5 h
NaCl	10	pH	5
GO	0.05	Temperature	25°C

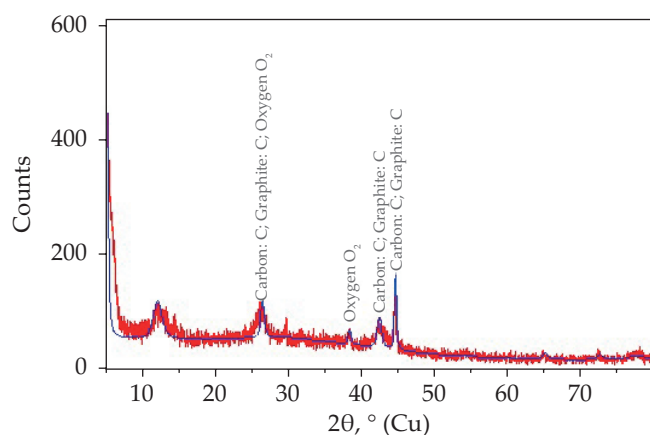


Fig. 4. XRD spectrum of graphite oxide obtained by Hummer's method

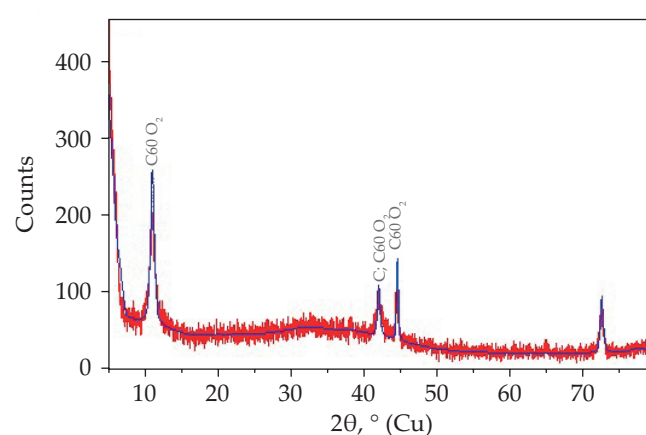


Fig. 5. XRD spectrum of graphene oxide obtained by modified Hummer's method

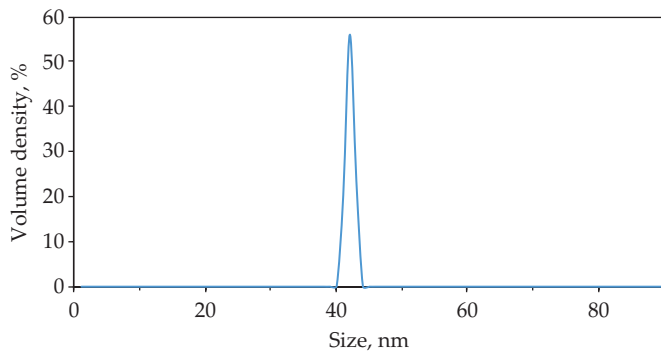


Fig. 6. Size distribution of GO particles obtained by modified Hummers' method

ite was oxidized in the presence of KMnO_4 and H_2SO_4 (Fig. 5). Sharp peaks at $2\theta = 41.93^\circ$ (d-spacing = 2.15 \AA) and $2\theta = 44.64^\circ$ (d-spacing = 2.03 \AA) indicate the presence of KMnO_4 [28]. The intensity of the diffraction peak at $2\theta = 41.93^\circ$ is much weaker than that at $2\theta = 44.64^\circ$. There was a very weak diffraction peak at $2\theta = 42.7^\circ$, which may indicate incomplete oxidation. There is also a sharp diffraction peak at $2\theta = 11.56^\circ$ with an interlayer distance of 7.66μ . The peak at $2\theta = 42.43^\circ$ was assigned to unexfoliated graphene oxide sheets [29]. The standard diffraction peak of pure graphite is located around $2\theta = 26^\circ$ [29]. However in the presented modified Hummers' method no such peak was obtained because graphite was oxidized to graphene oxide. The appearance of a peak at $2\theta = 45^\circ$ and a peak at $2\theta = 75^\circ$, due to the complete oxidation of the product after chemical oxidation and exfoliation, which indicates an increase in the d-spacing (31). The average number of graphene layers and average crystallite size (D) of 77 nm were determined using the Debye-Scherrer equation from XRD analysis.

Laser particle analysis

The results show that GO was successfully synthesized from graphite using the modified Hummers' method.

The particle size of GO is in the range of $40\text{--}45 \text{ nm}$ (Fig. 6). The XRD and LPA results showed similar size range of GO [36].

Scratch test

A scratch test was used to determine the failure limit and strength of steel samples with a composite coating. Figure 7 shows optical microscope images of scratch marks on samples and their magnified view of the load at which chip failure occurs at different coating times.

The results of scratch test showed a significant increase in coating adherence with respect to the increase of time (Fig. 8). In this test the chipping load increases with the increase in coating time at provided parameters. The significant coefficient of determination ($R^2 = 0.87$) strengthen established findings that by increasing the time of coating, the thickness load for creating scratch also increases [33].

Vickers microhardness

The Vickers microhardness of A-36 steel samples coated with the composite increased as a function of the coating time (Fig. 9) [34, 35].

The deviations of surface strength and hardness of the coated samples were shown in Fig. 10. The obtained results showed the significantly increase in hardness and strength with increase in percentage of GO and time of deposition which was explicitly specifies the thickness of coating. The similar increase in hardness of coating was previously observed by the group of researchers for the case of chromium with GO [32, 35]. The significant coefficient of determination ($R^2 = 0.93$) strength the findings that increase in hardness of samples impart the superior mechanical properties in addition to enhanced corrosion resistance [34, 35] and provided the wear and tear and anti-corrosion behavior for engineering and oil and gas applications.

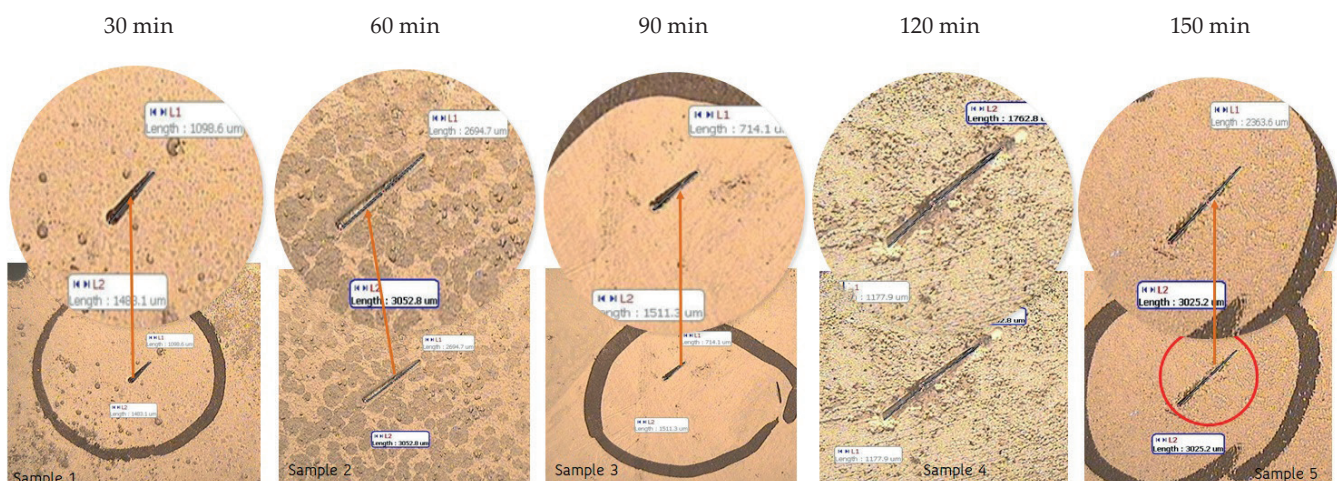


Fig. 7. Relation between coating time and failure load

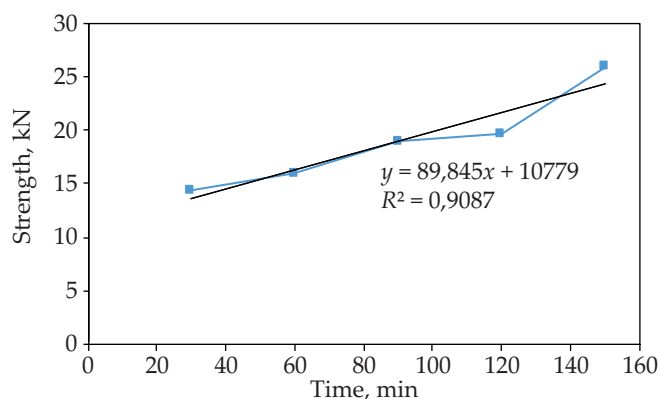


Fig. 8. Relation between coating time and failure load

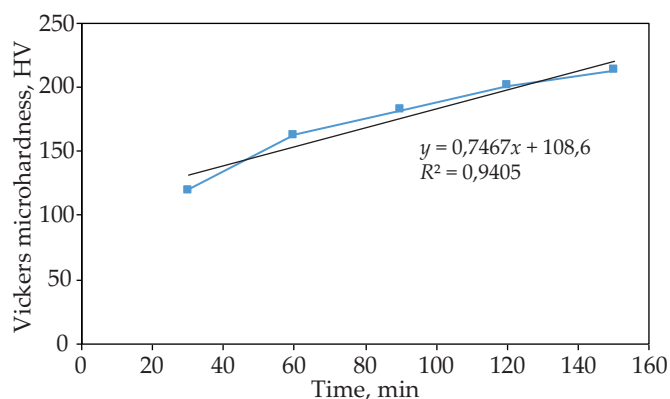


Fig. 10. Vickers microhardness as a function of coating time

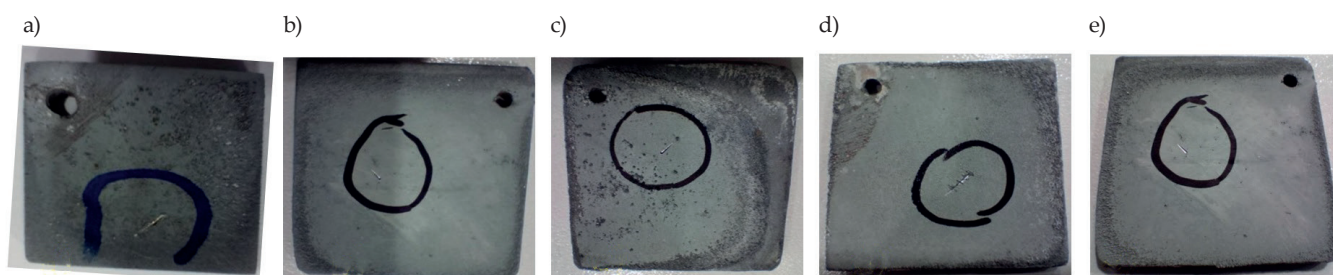


Fig. 9. Steel samples coated with Zn-GO differing in coating time: a) 30 min, b) 60 min, c) 90 min, d) 120 min, e) 150 min

CONCLUSIONS

Graphene oxide nanoparticles were synthesized using the modified Hummers' method, and XRD and LPA results showed that the size of the nanoparticles is less than 90 nm. The zinc-graphene nanocomposite coating was successfully applied by electrophoretic deposition. The results of the scratch hardness and Vickers microhardness tests showed improved mechanical properties of Zn-GO-coated A-36 steel samples, characterized by good durability and improved corrosion resistance in the harsh conditions of oil and gas pipelines.

ACKNOWLEDGMENT

Authors would like to acknowledge and appreciate kind support provided by NED University of Engineering and Technology, Pakistan.

REFERENCES

- [1] Azam A, Shafique M.: *International Journal of Advanced Science and Technology* **2017**, 103, 47. <https://doi.org/10.14257/ijast.2017.103.05>
- [2] Ossai C.I.: *International Scholarly Research Notices* **2012**, 2012, 1. <https://doi.org/10.5402/2012/570143>
- [3] Hernandez-Rodriguez M.A.L., Martinez-Delgado D., Gonzalez R. *et al.*: *Wear* **2007**, 263(1–6), 567. <https://doi.org/10.1016/j.wear.2007.01.123>
- [4] Ossai C.I., Boswell B., Davies I.J.: *Engineering Failure Analysis* **2015**, 53, 36. <https://doi.org/10.1016/j.engfailanal.2015.03.004>
- [5] Watts M.: "Curse of the black gold" powerHouse Books, Brooklyn 2010. p. 36.
- [6] Dai L., Wang D., Wang T. *et al.*: *Journal of Petroleum Engineering* **2017**, 2017, Article ID 3174636. <https://doi.org/10.1155/2017/3174636>
- [7] Adegboye M.A., Fung W.-K., Karnik A.: *Sensors* **2019**, 19(11), 2548. <https://doi.org/10.3390/s19112548>
- [8] Zhang X., Jing Q., Ao S. *et al.*: *Small* **2020**, 16(15), 1902820. <https://doi.org/10.1002/sml.201902820>
- [9] Singh Raman R.K., Chakraborty Banerjee P., Lobo D.E. *et al.*: *Carbon* **2012**, 50(11), 4040. <https://doi.org/10.1016/j.carbon.2012.04.048>
- [10] Cui G., Bi Z., Zhang R. *et al.*: *Chemical Engineering Journal* **2019**, 373(1), 104. <https://doi.org/10.1016/j.cej.2019.05.034>
- [11] Asim N., Badii M., Samsudin N.A. *et al.*: *Composites Part B: Engineering* **2022**, 245, 110188. <https://doi.org/10.1016/j.compositesb.2022.110188>
- [12] Freise E.J.: *Nature* **1962**, 193, 671. <https://doi.org/10.1038/193671a0>
- [13] Zhen Z., Zhu Z.: "Structure and Properties of Graphene" in "Graphene. Fabrication, Characterization, Properties and Applications" Academic Press, Elsevier 2017, p. 1.
- [14] Luo K., Liu B., Hu W. *et al.*: *Nature* **2022**, 607, 486. <https://doi.org/10.1038/s41586-022-04863-2>
- [15] Pajkossy T., Jurczakowski R.: *Current Opinion in Electrochemistry* **2017**, 1(1), 53. <https://doi.org/10.1016/j.coelec.2017.01.006>
- [16] Hares E., El-Shazly A.H., El-Kady M.F., Hammad A.S.: *Arabian Journal for Science Engineering* **2019**, 44, 5559.

- <https://doi.org/10.1007/s13369-019-03872-0>
- [17] Zhang X., Si Y., Mo J., Guo Z.: *Chemical Engineering Journal* **2017**, 313, 1152.
<https://doi.org/10.1016/j.cej.2016.11.014>
- [18] Bourell D., Kruth J.P., Leu M. *et al.*: *CIRP Annals* **2017**, 66(2), 659.
<https://doi.org/10.1016/j.cirp.2017.05.009>
- [19] Rekha M.Y., Srivastava C.: *Corrosion Science* **2019**, 152, 234.
<https://doi.org/10.1016/j.corsci.2019.03.015>
- [20] Zhu Y.X., Duan C.Y., Liu H.Y. *et al.*: *Journal of Physics D: Applied Physics*, **2017**, 50(11), 114001.
<https://doi.org/10.1088/1361-6463/aa5bb0>
- [21] Chiong S.J., Goh P.S., Ismail A.F.: *Journal of Natural Gas Science Engineering* **2017**, 42, 190.
<https://doi.org/10.1016/j.jngse.2017.02.042>
- [22] Kuilla T., Bhadra S., Yao D. *et al.*: *Progress in Polymer Science* **2010**, 35(11), 1350.
<https://doi.org/10.1016/j.progpolymsci.2010.07.005>
- [23] Van der Biest O.O., Vandeperre L.J.: *Annual Review of Materials Science* **1999**, 29(1), 327.
<https://doi.org/10.1146/annurev.matsci.29.1.327>
- [24] Besra L., Liu M.: *Progress in Materials Science* **2007**, 52(1), 1.
<https://doi.org/10.1016/j.pmatsci.2006.07.001>
- [25] Prasai D., Tuberquia J.C., Harl R.R. *et al.*: *ACS Nano* **2012**, 6(2), 1102.
<https://doi.org/10.1021/nn203507y>
- [26] Bannov A.G., Manakhov A., Shibaev A.A. *et al.*: *Thermochimica Acta* **2018**, 663, 165.
<https://doi.org/10.1016/j.tca.2018.03.017>
- [27] Sun L.: *Chinese Journal of Chemical Engineering* **2019**, 27(10), 2251.
<https://doi.org/10.1016/j.cjche.2019.05.003>
- [28] Yogesh G.K., Shuaib E.P., Roopmani P. *et al.*: *Diamond and Related Materials* **2020**, 104, 107733.
<https://doi.org/10.1016/j.diamond.2020.107733>
- [29] Pareek A., Shanthi Sravan J., Venkata Mohan S.: *Journal of Materials Science* **2019**, 54, 11604.
<https://doi.org/10.1007/s10853-019-03718-y>
- [30] Harris Z.D., Burns J.T.: *Corrosion Science* **2022**, 201, 110267.
<https://doi.org/10.1016/j.corsci.2022.110267>
- [31] Ambade S., Tembhurkar C., Patil A., Meshram D.B.: *World Journal of Engineering* **2022**, 19(3), 368.
<https://doi.org/10.1108/wje-11-2020-0591>
- [32] Jaworski S., Wierzbicki M., Sawosz E. *et al.*: *Nanoscale Research Letters* **2018**, 13, 1.
<https://doi.org/10.1186/s11671-018-2533-2>
- [33] Shakiba S., Khabbazi N.S., Tabrizi A.T., Aghajani H.: *Surface Engineering Applied Electrochemistry* **2022**, 58(2), 202.
<https://doi.org/10.3103/s1068375522020107>
- [34] Enani J.: *International Journal of Scientific Engineering Research* **2016**, 7(4), 1161.
<https://doi.org/10.47939/et.v1i1.27>
- [35] Kwak K., Mine Y., Morito S. *et al.*: *Materials Science Engineering: A* **2022**, 856, 144007.
<https://doi.org/10.1016/j.msea.2022.144007>
- [36] Amir M., Ahmed K., Hasany S.F., Butt R.A.: *AATCC Journal of Research* **2023**, 0, 0.
<https://doi.org/10.1177/24723444231161742>

Received 21 VI 2023

